Published in final edited form as:
Neuron. 2012 March 8; 73(5): 925–940. doi:10.1016/j.neuron.2011.12.037.

CYSL-1 Interacts with the O_2-sensing Hydroxylase EGL-9 to Promote H_2S-modulated Hypoxia-induced Behavioral Plasticity in *C. elegans*

Dengke K. Ma[1], **Roman Vozdek**[2], **Nikhil Bhatla**[1], and **H. Robert Horvitz**[1,*]

[1]Howard Hughes Medical Institute, Department of Biology, and McGovern Institute for Brain Research, MIT, Cambridge, MA 02139, USA.

[2]Institute of Inherited Metabolic Disorders, First Faculty of Medicine, Charles University in Prague and General University Hospital in Prague, Ke Karlovu 2, Prague 2, 128 08 Czech Republic.

SUMMARY

The *C. elegans* HIF-1 proline hydroxylase EGL-9 functions as an O_2-sensor in an evolutionarily conserved pathway for adaptation to hypoxia. H_2S accumulates during hypoxia and promotes HIF-1 activity, but how H2S signals are perceived and transmitted to modulate HIF-1 and animal behavior is unknown. We report that the experience of hypoxia modifies a *C. elegans* locomotive behavioral response to O_2 through the EGL-9 pathway. From genetic screens to identify novel regulators of EGL-9-mediated behavioral plasticity, we isolated mutations of the gene *cysl-1*, which encodes a *C. elegans* homolog of sulfhydrylases/cysteine synthases. Hypoxia-dependent behavioral modulation and H_2S-induced HIF-1 activation require the direct physical interaction of CYSL-1 with the EGL-9 C-terminus. Sequestration of EGL-9 by CYSL-1 and inhibition of EGL-9-mediated hydroxylation by hypoxia together promote neuronal HIF-1 activation to modulate behavior. These findings demonstrate that CYSL-1 acts to transduce signals from H2S to EGL-9 to regulate O_2-dependent behavioral plasticity in *C. elegans*.

INTRODUCTION

Oxygen (O_2) is essential for most life forms. An abnormally low level of O_2, or hypoxia, affects diverse biological processes, including embryonic development, physiological homeostasis and behavioral adaptation, as well as many pathological conditions, such as ischemic stroke, neurodegeneration, tumor formation and metastasis (Kaelin and Ratcliffe, 2008; Semenza, 2010). Evolutionarily conserved proline-4-hydroxylase domain enzymes have been identified as intracellular receptors for O_2 (Bruick and McKnight, 2001; Epstein et al., 2001; Ivan et al., 2002). Under normal conditions, PHDs use O_2 as a substrate to hydroxylate the transcription factor hypoxia inducible factor (HIF). Hydroxylated HIF is recognized by the von Hippel-Lindau (VHL) tumor suppressor protein, a component of an

*Correspondence horvitz@mit.edu; Phone: (617) 253-4671.

SUPPLEMENTAL INFORMATION
Supplemental Information includes seven figures and one table

CONFLICT OF INTEREST
The authors declare no financial conflicts of interest.

E3-ubiquitin ligase complex that targets HIF for proteosomal degradation. Under hypoxic conditions, impaired PHD protein function leads to up-regulation of HIF and its target gene expression. Mutations in the human HIF PHD enzyme, EGLN2, can cause congenital erythrocytosis (Percy et al., 2006) and possibly recurrent paragangliomas (Ladroue et al., 2008). With central roles in many human biological processes, HIF PHDs are promising therapeutic targets for treating ischemic stroke, neurodegenerative diseases and cancer (Mazzone et al., 2009; Quaegebeur and Carmeliet, 2010). The first O_2-sensing PHD enzyme identified was the *C. elegans* EGL-9 protein, the product of a gene defined by mutations that cause an egg-laying behavioral defect (Darby et al., 1999; Epstein et al., 2001; Trent et al., 1983).

C. elegans exhibits diverse genetically tractable behaviors that are regulated by internal physiological states, environmental cues, and behavioral experiences (de Bono and Maricq, 2005; Jorgensen and Rankin, 1997; Sawin et al., 2000). Studies of several *C. elegans* behaviors have significantly increased our understanding of the molecular and neural mechanisms underlying behavioral plasticity, a major problem in neurobiology. *C. elegans* naturally lives in soil or in microbe-rich habitats where O_2 is usually reduced from the ambient level of 21% (Felix and Braendle, 2010) and prefers hypoxic ranges of O_2 concentration when tested in laboratory aerotaxis experiments (Gray et al., 2004). Prior experience of hypoxia can activate HIF-1 and shift the animal's O_2 preference towards lower O_2 levels (Chang and Bargmann, 2008; Cheung et al., 2005). Hypoxia also enhances NaCl chemotaxis through HIF-1-dependent up-regulation of TPH-1, a biosynthetic enzyme for the neural modulator serotonin (Pocock and Hobert, 2010). While the EGL-9 pathway chronically monitors O_2 changes to elicit behavioral plasticity through transcriptional regulation, acute sensing of O_2 at levels ranging from 4%–21% is mediated by soluble guanylate cyclase (GCY) family proteins (Cheung et al., 2004; Gray et al., 2004; McGrath et al., 2009; Zimmer et al., 2009).

The evolutionarily conserved EGL-9/HIF-1 pathway is highly regulated to dynamically control the expression of many genes important for hypoxic adaptation (Powell-Coffman, 2010). As 2-oxoglutarate-dependent dioxygenases with Fe^{2+} and ascorbate as co-factors, HIF PHDs are sensitive to ambient O_2 levels as well as to fluctuations in cell metabolic and redox status (Rose et al., 2011). In *C. elegans*, EGL-9 destabilizes HIF-1 via its hydroxylation and subsequent degradation by the VHL-1 complex and also inhibits HIF-1 transcriptional activity through unidentified hydroxylation-independent mechanisms (Shao et al., 2009). Similar dual-mode inhibition of HIF has been observed for mammalian HIF PHDs (Ozer et al., 2005; To and Huang, 2005). In addition, the *C. elegans* protein RHY-1 inhibits HIF-1 independently of VHL-1 (Shen et al., 2006), although the relationship between RHY-1 and EGL-9 and the mechanism by which RHY-1 inhibits HIF-1 remain to be established.

Hydrogen sulfide (H_2S), which is endogenously synthesized by many organisms, has recently emerged as a gaseous cell signaling molecule and neuromodulator involved in numerous biological processes. In mammals, H_2S critically affects dilation of blood vessels, hippocampal long-term potentiation, ischemia/reperfusion injury response, cell protection from oxidative stresses and neurodegenerative disorders, including Alzheimer's and Parkinson's disease (Gadalla and Snyder, 2010; Kimura, 2010; Li et al., 2011; Szabo, 2007). H_2S levels increase under hypoxic conditions and can mediate hypoxic effects on vasodilation and ventilatory responses (Olson et al., 2006; Peng et al., 2010). In *C. elegans*, exposure to H_2S activates HIF-1 and promotes survival of animals during H_2S exposure (Budde and Roth, 2010). H_2S also activates HIF in mammalian cells (Liu et al., 2010). How H_2S signals are perceived and transmitted to activate HIF and whether H_2S interacts with HIF PHD enzymes to modulate animal behaviors are unknown.

To identify components of the *egl-9/hif-1* pathway, we conducted a series of genetic screens and recovered mutations of *egl-9*, *hif-1*, *rhy-1* and the gene *cysl-1*. A recent study found that *cysl-1* mutants are sensitized to H2S toxicity via an unknown mechanism (Budde and Roth, 2011). We demonstrate that CYSL-1 acts upstream of HIF-1 as a signal transduction protein that directly binds to the EGL-9 proline hydroxylase in a H_2S-modulated manner and prevents EGL-9 from inhibiting HIF-1. We show that RHY-1, CYSL-1 and EGL-9 act in a cascade to control HIF-1 activity and modulate locomotive behavioral responses to changes in O_2 levels. *cysl-1* apparently evolved from an ancient metabolic cysteine synthase gene family, and the emergence of novel *cysl-1* functions in cell signaling exemplifies an intriguing case of gene "cooption" (True and Carroll, 2002) during genome evolution for adaptation to changing environmental conditions.

RESULTS

C. elegans exhibits locomotive behavioral plasticity in response to the experience of hypoxia

O_2 availability pervasively influences *C. elegans* physiology and behavior, providing rich avenues to dissect fundamental molecular and neural mechanisms for behavioral plasticity. We developed a custom-built multi-worm tracker with a computer-controlled gas-flow system (Figure S1A) to seek robust and novel *C. elegans* behaviors. We focused on the locomotion of adult *C. elegans* hermaphrodites (of the laboratory wild-type Bristol strain N2) in response to step changes of O_2 between 20% and 0% (anoxia). We measured the animals' mean locomotion speed and turning angle in the presence of bacterial food after we shifted O_2 concentration between 20% and 0% ("O2-OFF") and between 0% and 20% ("O2-ON"). Reducing O_2 caused a transient increase in locomotion speed and turning angle (Figures 1A, 1B and S1B). The O2-OFF response resembled the previously reported local search behavior induced by food withdrawal (Gray et al., 2005) and lasted for about one minute after anoxia exposure.

With prolonged exposure to anoxia, animals eventually enter a state of suspended animation (Padilla et al., 2002). To examine the acute behavioral response to O_2 restoration, we returned the environment to 20% O_2 after five minutes of anoxia exposure. Animals responded to the acute elevation of O_2 with a dramatic acceleration of locomotion speed, which we defined as the "O2-ON" response (Figures 1A, 1B and S1B). The O2-ON response was caused specifically by anoxia/reoxygenation (Figures 1A and S1H) and might reflect an aversive behavior to unfavorable anoxia/reoxygenation signals. The O2-ON response was also observed for animals under conditions without bacterial food, for the Hawaiian strain CB4856, and in response to smaller increases in O_2 levels (from 0% to 5% or 10%) (Figures S1B–S1F). These results identify the O2-ON response as a previously uncharacterized acute locomotive response induced by rapid and large increases in O_2 levels.

To examine whether prior prolonged exposure to hypoxia would modify the O2-ON response, we cultured adult hermaphrodites at 0.5% O_2 for 24 hrs, allowed them to recover for 2 hrs in room air, and then tested them in our behavioral assay (Figure 1C). The hypoxia-experienced animals had an essentially normal O2-OFF response, while their O2-ON response was strikingly decreased, with a negligible acceleration in response to O_2 elevation (Figure 1D). To test how long the effects of hypoxia exposure last, we varied the duration of recovery after 24 hours of hypoxia exposure and found significant inhibition of O2-ON response for at least 8 hours after the hypoxia exposure (Figure S1I). To test how long hypoxia exposure is needed for such behavioral modification, we varied the duration of hypoxia experience and found that at least 16 hours of 0.5% O_2 were required to elicit complete inhibition of the O2-ON response (Figure S1J). These data suggest that inhibition

of the O2-ON response requires prolonged prior hypoxia experience and can be long-lasting, representing a type of behavioral plasticity.

EGL-9 and HIF-1 mediate the hypoxia-induced reduction of the O2-ON response

Since EGL-9 has been identified as the chronic O2 sensor in *C. elegans* and HIF-1 has been implicated in other types of hypoxia-induced behavioral plasticity (Chang and Bargmann, 2008; Epstein et al., 2001; Pocock and Hobert, 2010), we examined *egl-9* and *hif-1* null mutants in our behavioral assays. Strikingly, mutations of *egl-9* caused the animals to be completely defective in the O2-ON response (Figures 1E, S2A). *egl-9* mutants accumulate constitutively active forms of HIF-1 (Epstein et al., 2001; Shao et al., 2009), so we postulated that the *egl-9* phenotype we observed reflect the hypoxia-mimicking effects of *egl-9* mutants that result from constitutive activation of HIF-1. Indeed, we found that *egl-9; hif-1* double mutants displayed a fully restored O2-ON response (Figure 1F). *hif-1* single mutants are severely defective in the hypoxia-induced inhibition of the O2-ON response (Figure 1G), while normal in the acute O2-OFF and O2-ON responses (Figure 1H). We found normal O2-ON responses by *tph-1*, *gcy-31*, *gcy-33*, *gcy-35*, *gcy-36*, *mbk-1*, *swan-1* mutants and by a strain with apoptotic cell deaths of the URX, AQR and PQR neurons (*qaIs2241*); these strains were previously implicated in EGL-9 or O_2-dependent responses (Chang and Bargmann, 2008; Pocock and Hobert, 2010; Shao et al., 2010; Zimmer et al., 2009) (Figures S2B–S2H). Together, these results suggest that the experience of hypoxia inactivates EGL-9, leading to HIF-1 activation and hypoxia-induced inhibition of the O2-ON response.

RHY-1 is a positive regulator of EGL-9 and the O2-ON response

To determine how EGL-9 is modulated to control the O2-ON behavior, we screened for mutants that resembled *egl-9* mutants. To facilitate this screen, we constructed an integrated transgenic reporter strain (*nIs470*) in which a green fluorescent protein (GFP) variant (Venus) was driven by the promoter of a known HIF-1 target gene, *K10H10.2* (Shen et al., 2006). *egl-9* mutants exhibited bright GFP fluorescence throughout the animal, whereas GFP was essentially absent in *egl-9(+)* and *egl-9; hif-1* double mutants (Figure 2A), indicating that the GFP transgene specifically reports the transcriptional activity of HIF-1.

We used ethyl methansulfonate (EMS) to mutagenize the *egl-9(+)*; $P_{K10H10.2}$*::GFP* (*nIs470*) strain and sought for mutations that activate *K10H10.2::GFP* expression. From a screen of approximately 30,000 haploid genomes, we isolated four mutations that failed to complement *egl-9*, two that failed to complement *vhl-1*, and another two (*n5492* and *n5500*) that identified a third complementation group and were genetically linked to a 900-kb interval on chromosome II (Table S1A, and data not shown). We noticed that this interval contains the gene *rhy-1*, which had been implicated in HIF-1 regulation (Shen et al., 2006). We determined DNA sequences of the *rhy-1* coding region in *n5492* and *n5500* animals and found missense mutations in both (Figures S3A–S3C). The *n5500* and *n5492* alleles caused animals to express ectopic *K10H10.2::GFP* and to be defective in the O2-ON response in a HIF-1-dependent manner (Figures 2B–2D, data not shown). An extrachromosomal array with *rhy-1(+)* genomic DNA rescued the defects in both the O2-ON response and GFP expression (Figures 2E–2F). Furthermore, RNAi against *rhy-1* and a *rhy-1* null deletion allele *ok1402* conferred the same phenotype as that of *n5500* mutants (Figures 2G and S3D). We conclude that *n5492* and *n5500* are alleles of *rhy-1* and that *rhy-1* is necessary for the O2-ON response.

To define the genetic relationship of *rhy-1* to *egl-9* and *hif-1*, we performed epistasis analysis by constructing double loss-of-function (LOF) or gain-of-function (GOF) mutants. *hif-1* is epistatic to *rhy-1*, since *hif-1* LOF suppressed *rhy-1* LOF phenotypes (Figures 2B

and 2D). *egl-9* overexpression by an integrated transgene suppressed the *rhy-1* LOF phenotype of *K10H10.2::GFP* expression and the impaired O2-ON response, whereas *rhy-1* overexpression failed to suppress the corresponding *egl-9* LOF phenotype (Figure S3F and Table 1C). These data suggest a genetic pathway in which RHY-1 positively regulates EGL-9, which inhibits HIF-1 to regulate HIF-1 targets and behavior.

A *rhy-1(n5500)* suppressor screen identified *cysl-1* as a key regulator of EGL-9 and behavior

To identify the mechanism by which RHY-1 regulates EGL-9 and HIF-1, we performed a screen for suppressors of the ectopic expression of *K10H10.2::GFP* by *rhy-1*(*n5500*) mutants. From a screen of approximately 50,000 haploid genomes, we isolated 17 independent *n5500* suppressors that defined at least four genes (Table 1A). Two mutations failed to complement *hif-1* and restored the O2-ON response defects of *rhy-1(n5500)* animals. Mutations from the second complementation group caused reduced expression both of *K10H10.2::GFP* and of co-injection markers and are alleles of *tam-1*, which is known to be required for repetitive transgene expression (Hsieh et al., 1999). The third complementation group of seven alleles, including *n5515*, appeared to define a novel gene involved in HIF-1 regulation. We also isolated three *egl-9* alleles (*n5535*, *n5539* and *n5552*) that dominantly suppressed *rhy-1(n5500)*.

Three-factor mapping placed *n5515* between *dpy-6* and *egl-15* on chromosome X. Single nucleotide polymorphism (SNP) mapping using the Hawaiian strain further positioned *n5515* within a 0.28 map unit region. We used RNAi against candidate genes in this region and found that RNAi against a single gene, *C17G1.7 (cysl-1)*, fully recapitulated the *n5515* phenotype. Sequence determination revealed that all seven mutants contained mutations in the *cysl-1* coding region, including five missense transition mutations, one nonsense transversion mutation and a 330-bp deletion (*n5536*) (Figures 3A and S5C, Table 1B). Both *n5536* and another deletion allele of *cysl-1*, *ok762*, conferred the same phenotype as that of *n5515* mutants. Like *hif-1* alleles but unlike *tam-1* alleles, the *cysl-1* null alleles restored the O2-ON response defect of *rhy-1(n5500)* mutants (Table 1C, Figures 3B–3E, and data not shown).

To define the relationship of *cysl-1* with *egl-9*, *hif-1* and *rhy-1*, we performed epistasis analysis by constructing double mutants for individual pairs of *rhy-1*, *cysl-1*, *egl-9* and *hif-1* mutations (Table 1C). *hif-1* was epistatic to all three other genes. *egl-9* was epistatic to *cysl-1*, which was epistatic to *rhy-1* (Figures 3D–3G and Table 1C). Semi-quantitative measurements by western blots of GFP protein in various single or multiple mutants were consistent with phenotypic analyses of *K10H10.2::GFP* fluorescence levels and O2-ON responses, e.g. *cysl-1* completely suppressed *rhy-1* in GFP levels (Figure 3H). Furthermore, the endogenous expression of *K10H10.2* exhibited patterns of regulation similar to that of GFP driven by the *K10H10.2* promoter (Figure 3I). These results led us to suggest a genetic pathway in which *rhy-1* inhibits *cysl-1*, which inhibits *egl-9*, which inhibits *hif-1*, which promotes *K10H10.2* expression and inhibits the O2-ON response.

cysl-1 is expressed in and functions in neurons

To explore the function of CYSL-1 in HIF-1 regulation and behavioral modulation, we determined the expression pattern of *cysl-1* using an integrated transcriptional GFP reporter and an extrachromosomal translational GFP reporter. A 2.8 kb promoter of *cysl-1* drove GFP expression mainly in the nervous system of adult hermaphrodites (Figure 4A). The *cysl-1::GFP* expression pattern was similar for the transcriptional and translational reporters (Figures 4A–4E and S4A). GFP was observed in subsets of pharyngeal neurons, amphid sensory neurons and tail neurons, starting from late embryonic stages and persisting into

adults. We identified GFP-positive cells as the AVM sensory neuron, the BDU interneurons (Figure 4B) and the pharyngeal I1 interneurons and M2 motor neurons (Figure 4C), based on their characteristic processes and nuclear positions. GFP in body wall muscles, hypoderm and intestine was present in larvae but only weakly detectable in adult animals.

The neuronal expression pattern of *cysl-1* is consistent with its role in O2-ON behavioral modulation. However, *cysl-1* mutations suppressed ectopic *K10H10.2::GFP* expression in the hypoderm of *rhy-1* mutants (Figures 3C and S3B, Table 1B). To further examine the site-of-function of *cysl-1*, we generated transgenic strains harboring a wild-type *cysl-1* cDNA driven by the *ric-19* neural-specific promoter (Ruvinsky et al., 2007). *ric-19* promoter-driven neuronal expression of *cysl-1*, but not *dpy-7* promoter-driven hypodermal expression of *cysl-1*, rescued the O2-ON behavior of *rhy-1; cysl-1* double mutants (Figures 4F, 4G and S4B). Hypodermal expression of *cysl-1* rescued the *K10H10.2::GFP* expression of *rhy-1; cysl-1* mutants (Figure S4C). These data support the hypothesis that *cysl-1* functions in neurons to control HIF-1 activity for O2-ON behavioral modulation. We suggest that hypodermal *K10H10.2* expression reflects HIF-1 activation but is not functionally important for O2-ON behavioral modulation. In support of this notion, we found that *egl-9(−); K10H10.2 (−)* double mutants were defective in the O2-ON response, just as are *egl-9(−)* single mutants (Figure S4D). As an independent test of the importance of neuronal regulation of HIF-1 for O2-ON behavioral modulation, we introduced a stabilized form of the HIF-1 protein (P621A) into various tissues in the *egl-9; hif-1* double mutant background. Proline 621 of HIF-1 is the hydroxylation target of EGL-9, and the P621 mutant HIF-1 protein is enhanced in stability (Epstein et al., 2001; Pocock and Hobert, 2010). Stabilization of HIF-1 protein was not sufficient to cause a defect in the O2-ON response (Figure S4E), suggesting that additional P621 hydroxylation-independent activation of HIF-1 is required for suppressing the O2-ON response. This hypothesis is also consistent with the partially defective O2-ON response of *vhl-1(−)* mutants (Figure S2F). In the *egl-9; hif-1* background, neuronal expression of *hif-1*(P621A) driven by an *unc-14* promoter resulted in a defective O2-ON response (Figure 4H). By contrast, hypodermal expression of *hif-1*(P621A) driven by the *dpy-7* promoter or muscle-specific expression of *hif-1*(P621A) driven by the *unc-120* promoter did not cause a defective O2-ON response (Figures 4I and S4F). These results indicate a neuronal site-of-function of *cysl-1* in regulating the *egl-9/hif-1* pathway to modulate the O2-ON response.

cysl-1 encodes a member of an evolutionarily ancient cysteine synthase/sulfhydrylase gene family

We used BLASP to search the NCBI protein database and found many CYSL-1 homologs belonging to the cystathionine-beta synthase/cysteine synthase (CBS/CS) family of the fold type-II pyridoxal-5'-phosphate (PLP)-dependent proteins in diverse species ranging from bacteria to humans (Figures 5A and S5A). The *cysl-1(n5515)* allele we isolated from the *rhy-1(n5500)* suppressor screen converted glycine 183 to arginine (Figure 5A, Table 1B). Strikingly, this glycine is 100% conserved among the *cysl-1* homologs of all species examined (bacteria, yeast, flies, zebrafish, mice, and humans) and is positioned at the core of a motif sequence crucial for binding to the obligate co-factor PLP (Aitken et al., 2011) (Figures 5A and S6C). Interestingly, one of the CYSL-1 paralogs is the HIF-1 target gene *K10H10.2*, indicating a possible feedback regulation of this gene family. We raised a polyclonal CYSL-1 antibody and found reduced levels of steady-state CYSL-1(*n5515*) proteins in soluble fractions of *C. elegans* and bacterial homogenates compared to those of wild-type CYSL-1 (Figures 5B and S5B). The introduction at residue 183 of arginine, which has a long protruding hydrophilic side chain (Figure S6E), could disrupt binding to PLP and render the protein improperly folded and unstable. *n5521*, *n5522* and *n5537* mutants similarly showed reduced levels of CYSL-1 (Figures 5B and S5B, S6C–S6F).

We studied recombinant CYSL-1 proteins purified from *E. coli* and found that CYSL-1 exhibited properties typical of type-II PLP-dependent proteins (Figures S5D–S5G). We tested several biochemical reactions that had previously been associated with other PLP-dependent CBS enzymes and cysteine synthases (Aitken et al., 2011; Mozzarelli et al., 2011). While assays for O-phosphoserine sulfhydrylase, cyanoalanine synthase, and cystathionine beta-synthase failed to yield significant enzymatic activities, CYSL-1 exhibited activity as an O-acetylserine sulfhydrylase (OASS), converting OAS and sulfide into L-cysteine and acetate (Figures 5C and 5D). However, the Michaelis constant K_M for sulfide (4.2 mM) of purified CYSL-1 was at least an order of magnitude higher than those of *bona fide* cysteine synthases, CYSL-1 homologs from bacteria and plants (Figure 5E), suggesting that the cysteine synthase activity of CYSL-1 might be insignificant physiologically *in vivo* and dispensable for regulating the *egl-9/hif-1* pathway. *cysl-1(n5519)* mutations suppressed HIF-1 target expression and restored the O2-ON response of *rhy-1(n5500)* mutants, yet the CYSL-1(*n5519)* mutant protein, with the abnormal lysine (R259K) residue on its surface far from the active site (Figure S6F) exhibited levels of OAS sulfhydrylase activity similar to that of wild-type CYSL-1 (Figures S6A and S6B, Table 1B). Notably, the CYSL-1(*n5519*) mutant protein exhibited steady-state levels comparable to that of wild-type CYSL-1 (Figures 5B and S5B). We obtained four additional lines of evidence supporting the notion that CYSL-1 regulates the EGL-9 pathway as a cell-signaling mediator independently of its cysteine synthase activity. First, the *C. elegans* genome does not appear to encode any homologs of O-serine acetyltransferase (SAT), which is an obligate component of the cysteine synthase pathway in bacteria and plants (Mozzarelli et al., 2011; Wirtz and Droux, 2005). BLASTP searches of animal protein databases against bacterial or plant SAT protein queries yielded only three significant hits (E value<1e-30), in honey bees, *Xenopus* and *Caenorhabditis remanei*, respectively. However, all three lack the invariant C-terminal isoleucine essential for binding to OASS (Campanini et al., 2005; Francois et al., 2006; Mozzarelli et al., 2011), and no other *Caenorhabditis* species appeared in the search. Second, a potential bacterial source of OAS as a cysteine synthase substrate for CYSL-1 is unlikely, since feeding *rhy-1(n5500)* mutants on a *cysE*-deleted *E. coli* strain deficient in OAS synthesis did not rescue the *rhy-1(n5500)* phenotype (Figure S6H). Third, we found that a lysine in an otherwise highly conserved motif crucial both for binding SATs and for functional CS activity (Bonner et al., 2005) is a proline in CYSL-1 (Figure S6G). Fourth, we found that CYSL-1 directly interacts with the C-terminus of EGL-9 instead of forming a cysteine synthase complex via its active site, as shown and discussed below.

CYSL-1 interacts with EGL-9 to mediate H_2S-induced HIF-1 activation and behavioral plasticity

In our *rhy-1(n5500)* suppressor screen, we isolated three mutations (*n5535, n5539* and *n5552*) that strongly suppressed *K10H10.2::GFP* expression and the defective O2-ON response (Table 1A and Figure 6A). Linkage mapping placed *n5535* on the right arm of chromosome V close to *egl-9*, which prompted us to determine the sequence of the *egl-9* coding region of these mutants. We found that *n5535* animals carry a missense mutation that converts the EGL-9 C-terminal sequence EYYI to KYYI, while the *n5539* and *n5552* alleles alter a splicing donor and a splicing acceptor site, respectively, causing EGL-9 to be prematurely truncated near the EGL-9 C-terminus without affecting the O_2-sensing proline-hydroxylase domain (Figure 6B). We noticed that the EYYI sequence of EGL-9 resembles the C-terminal SAT sequence DYVI, which penetrates into the active site of OASS, the CYSL-1 homolog in *Arabidopsis* (Francois et al., 2006). These observations, together with the dominant nature of the *n5535* phenotype and our epistasis analysis indicating that CYSL-1 inhibits EGL-9, suggested that *n5535* might disrupt an EGL-9-interacting interface with CYSL-1 and in that way dominantly suppress *rhy-1* LOF phenotypes.

To test directly whether CYSL-1 binds to the EGL-9 C-terminus, we generated a series of *egl-9* mutant constructs and analyzed them in a yeast two-hydrid assay. In this assay, EGL-9 proteins without the N-terminal zinc-finger domain specifically associated with CYSL-1, while the C-terminus alone or the full-length protein exhibited non-specific activation of the assay reporter without CYSL-1 (Figure 6C and data not shown). A five-amino acid deletion of the EGL-9 C-terminus (*egl-9* ΔPEYYI) abolished the specific interaction between EGL-9 and CYSL-1. Furthermore, EGL-9(*n5535*) mutant proteins harboring an E720K substitution near the C-terminus, or C-terminally truncated proteins caused by *n5539*, completely failed to interact with CYSL-1. We also probed the CYSL-1 interaction with EGL-9 using an independent fluorometric assay previously used to demonstrate direct peptide interactions between OASS and SAT proteins (Campanini et al., 2005; Francois et al., 2006). Wild-type EGL-9 C-terminal peptides with the last four, 10, or 14 amino acid residues significantly enhanced the intrinsic fluorometric emission of CYSL-1 in a dose-dependent manner (Figures S7A–S7D). Such enhancements were completely abolished for mutant peptides in which either the terminal isoleucine residue was substituted with alanine or the glutamic acid residue was substituted with lysine, as in *egl-9(n5535)* mutants (Figures S7E and S7F). These results demonstrated direct association between CYSL-1 and EGL-9 specifically mediated by the C-terminal residues of EGL-9.

Because CYSL-1, with its presumptive evolutionary origin from sulfide metabolism pathways, is associated with the EGL-9 C-terminus and our genetic analysis identified CYSL-1 as a negative regulator of EGL-9, we wondered whether CYSL-1 might transduce signals from H_2S to the HIF-1 transcriptional pathway through EGL-9 inhibition. To test this hypothesis, we first confirmed previous findings that low nonlethal exposure of H_2S can activate HIF-1 as assayed by *K10H10.2::GFP* expression and by real-time RT-PCR analysis of two different HIF-1 target genes, *K10H10.2* and *nhr-57* (Figures 6D–6F). We found that the strong induction of *K10H10.2* and *nhr-57* in response to H_2S exposure was strikingly absent in *cysl-1* mutants and also in *egl-9(n5535)* mutants containing the E720K mutation, which selectively disrupts the interaction between CYSL-1 and EGL-9 (Figures 6D–6F). Although H_2S exposure can activate the HIF-1 target genes *K10H10.2* and *nhr-57*, it was not sufficient to inhibit the O2-ON response (Figures S7G). H_2S was previously shown to up-regulate HIF-1 activity independently of VHL-1 (Budde and Roth, 2010), indicating that HIF-1 protein stabilization acts in parallel with H_2S exposure for enhanced HIF-1 activation. Supporting this notion, we found that H_2S elicited inhibition of the O2-ON response in animals (*otIs197 [*$P_{unc\text{-}14}$*::hif-1P621A]*) harboring the stabilized mutant P651A HIF-1 protein in neurons (Figures S7G–S7I). Furthermore, exposure to H2S markedly enhanced the interaction between CYSL-1 and EGL-9 *in vivo* (Figure 6G). These data indicate that CYSL-1 and its interaction with the EGL-9 C-terminus are crucial for activation of HIF-1 targets in response to H_2S exposure and that this mechanism acts together with EGL-9-mediated HIF-1 hydroxylation to regulate HIF-1 and modulate the O2-ON response.

Because hypoxia promotes H_2S accumulation (Olson, 2011; Olson et al., 2006; Peng et al., 2010), we directly tested whether the experience of hypoxia requires CYSL-1 to modulate the *egl-9/hif-1* pathway and the O2-ON behavioral response. Unlike wild-type animals, which exhibited robust hypoxia experience-induced inhibition of the O2-ON response, *cysl-1* mutants were defective in such behavioral plasticity (Figure 6H). Naïve wild-type animals and *cysl-1* mutants without prior hypoxia experience were both normal in the O2-ON response (Figures 1A and 3F). Furthermore, *egl-9(n5535)* mutants, in which the E720K mutation disrupts interaction with CYSL-1, were defective in the hypoxia-induced inhibition of the O2-ON response (Figure 6I). These results demonstrate that CYSL-1 and its interaction with EGL-9 are essential for hypoxia experience-dependent inhibition of the O2-ON response.

DISCUSSION

Our studies have identified a novel behavioral plasticity of *C. elegans*, delineated a genetic pathway for its regulation (Figure 7A), discovered CYSL-1 from a genetic screen as a key component of this pathway, and elucidated essential roles of the interaction between CYSL-1 and EGL-9 in mediating H2S signaling to HIF-1 and for hypoxia experience-dependent behavioral modulation (Figures 7B–7C). Our combined genetic, biochemical and behavioral data support the following model. Under conditions of no prior experience of hypoxia, EGL-9 inhibits both the stability (via hydroxylation) and the transcriptional activity of HIF-1 to allow a robust O2-ON locomotive behavioral response; RHY-1 negatively regulates CYSL-1 to prevent it from inhibiting EGL-9 (Figure 7B). Under hypoxic conditions, decreased O_2 levels cause impaired EGL-9 hydroxylase activity and consequent stabilization of the HIF-1 protein; H_2S, endogenously and/or from local environments accumulates during prolonged hypoxia and promotes the interaction of EGL-9 and CYSL-1, which sequesters EGL-9 and thus prevents EGL-9 from inhibiting the transcriptional activity of HIF-1; together, EGL-9 sequestration by CYSL-1 and hypoxia-induced impairment of the hydroxylase activity of EGL-9 drive activation of neuronal HIF-1 target genes to coordinate a transcriptional program that culminates in inhibition of the O2-ON response (Figure 7C).

The O2-ON response occurs within a brief window (< 30 seconds), which might reflect a rapid aversive behavioral response to unfavorable anoxia/reoxygenation signals, whereas the EGL-9-mediated O_2-sensing mechanism operates during a much longer period (24 hours) of hypoxia exposure (Figures 1A–1H). Several neurons (URX, AQR, PQR, BAG) and specific guanylate cyclases have been identified as O_2 sensors for hyperoxia avoidance (10% to 20% O2) in *C. elegans* (Cheung et al., 2004; Gray et al., 2004; Zimmer et al., 2009), but the O2-ON behavior appears to depend on distinct O_2 sensors (0% to 5% and 20% O2) and neural mechanisms (Figures S1G and S2B–S2G). In contrast to naïve animals, hypoxia-experienced animals suppress the subsequent O2-ON response and do so in a manner that depends on HIF-1 activation of target genes in neurons (Figures 4F–4I), and the behavioral effect can last for up to 8 hours after the initial trigger stimulus of 24 hrs of hypoxia (Figures S1I and S1J). Such experience-dependent persistent neural modification might represent a behavioral plasticity that acts as a gain-control mechanism to dampen neural responses to strong environmental stimuli (Demb, 2008). The experience of hypoxia might also produce pre-conditioning effects and reduce the O2-ON response to anoxia/reoxygenation-induced cellular signals.

Our studies and those of others (Chang and Bargmann, 2008; Cheung et al., 2005; Pocock and Hobert, 2010) demonstrate that HIF-1 plays crucial roles in hypoxia experience-dependent *C. elegans* behavioral modifications. We identified a novel genetic pathway that regulates HIF-1 and hypoxia-induced behavioral plasticity (Figure 7A). What are the underlying molecular mechanisms? RHY-1 is an endoplasmic reticulum acyltransferase-like protein (Figure S3C) and appears to down-regulate the abundance of CYSL-1 protein (Figure 5B). One possibility is that RHY-1 promotes CYSL-1 N-terminal acetylation, a modification known to alter plant CYSL-1-like sulfhydrylases (Wirtz et al., 2010), and in this way also promotes CYSL-1 degradation (Hwang et al., 2010). All three *egl-9* alleles isolated from our *rhy-1(n5500)* suppressor screen disrupt the EGL-9 C-terminus without affecting the O_2-sensing PHD domain, suggesting that CYSL-1 sequestration of EGL-9 operates in parallel to EGL-9 hydroxylation of HIF-1 and that EGL-9 regulates HIF-1 at two different levels. Specifically, hypoxia might activate HIF-1 both by causing CYSL-1-mediated sequestration of EGL-9 and by preventing O_2-stimulated HIF-1 degradation. Under normoxic conditions, EGL-9 might act in part through SWAN-1 and MBK-1 (Shao et al., 2010) independently of RHY-1 and CYSL-1 to inhibit HIF-1 transcriptional activity. Such dual-mode EGL-9 inhibition of HIF-1 is consistent with previous studies of *C. elegans*

and mammalian cells indicating that EGL-9-like HIF proline hydroxylases inhibit HIF proteins through both enzymatic hydroxylation to decrease HIF protein stability and non-enzymatic suppression of HIF transcriptional activities (Ozer et al., 2005; Shao et al., 2009; To and Huang, 2005). However, in previous studies (Budde and Roth, 2010; Shen et al., 2005) hypoxia has not fully mimicked the effects of EGL-9 inactivation and it has been unclear whether or not the second EGL-9 pathway mediates a response to hypoxia. Importantly, we found that sufficient hypoxia can fully mimic the suppressed O2-ON response in *egl-9* mutants (Figures 1D and 1E), indicating that hypoxia indeed not only stabilizes HIF-1 but also acts via CYSL-1 and H_2S to facilitate HIF-1 transactivation for modulation of the O2-ON response.

In vertebrates, H_2S drastically increases under hypoxic conditions to levels that are inversely correlated with tissue O_2 levels (Olson, 2011; Olson et al., 2006; Peng et al., 2010). H_2S is endogenously produced by multiple types of enzymes in animals and is constantly oxidized, so its increase might be directly regulated by local O_2 levels to mediate effects of hypoxia (Chen et al., 2004; Kimura, 2010; Olson, 2011; Peng et al., 2010; Singh et al., 2009). In both *C. elegans* and mammalian cells, H_2S has been shown to promote HIF-1 activity and up-regulate HIF-1 target genes (Budde and Roth, 2010; Liu et al., 2010). However, the mechanism by which H_2S elicits its effects on HIF-1 has been unknown. Our findings demonstrate an essential role of CYSL-1 in mediating H_2S up-regulation of HIF-1 target genes through CYSL-1 interaction with the EGL-9 C-terminus. A recent study found that *cysl-1* mutants are sensitive to H_2S and hypothesized that CYSL-1 might act in a pathway downstream of HIF-1 to enzymatically assimilate H_2S (Budde and Roth, 2011). Unexpectedly, our studies show that CYSL-1 acts upstream of HIF-1 by directly inhibiting EGL-9 in a manner that is modulated by H_2S accumulation. Interestingly, both H_2S and RHY-1 appear to regulate HIF-1 activity in a VHL-1-independent manner (Budde and Roth, 2010; Shen et al., 2006), consistent with the notion that CYSL-1 inhibits EGL-9 and mediates H_2S activation of HIF-1 independently of EGL-9 hydroxylase activity. Bisulfide is known to bind to an allosteric regulatory site of *Salmonella* OASS proteins, which are highly similar to CYSL-1 in *C. elegans*, and can stabilize the interaction between OASS and the SAT C-terminus (Salsi et al., 2010). H_2S inhibits mitochondrial cytochrome-C oxidase and can also directly modify target proteins via sulfhydration (Mustafa et al., 2009). Although CYSL-1 has only weak intrinsic sulfhydrylase activity *in vitro*, it remains possible that H_2S might modify EGL-9 via CYSL-1-modulated sulfhydration to facilitate sequestration of EGL-9 by CYSL-1. The detailed mechanism by which H_2S and its *in vivo* derivatives modulate CYSL-1 and EGL-9 to regulate HIF-1 remains to be investigated.

CYSL-1-homologous CBS proteins in mammals are known to be major H_2S-biosynthetic enzymes (Chen et al., 2004; Singh et al., 2009), and we suggest that the pathway we identified is fundamentally similar in nematodes and mammals (Figure 7A). In nematodes, H_2S and CYSL-1 regulate HIF-1 through EGL-9. In mammals, H2S also regulates HIF proteins (Li et al., 2011; Liu et al., 2010), and we propose that CYSL-1-like CBS proteins generate endogenous H_2S to modulate HIF. In mammals, HIF activation protects tissues from reperfusion injury (Loor and Schumacker, 2008); we propose that the *C. elegans* O2-ON behavior reflects an aversive response to unfavorable reoxygenation signals, and is analogous to reperfusion injury in mammals. Just as *C. elegans* HIF-1 activates a set of target genes, mammalian HIF can activate *VEGF* to promote tumor angiogenesis (Kaelin and Ratcliffe, 2008; Semenza, 2010). Given that HIF proline hydroxylases and H_2S are emerging as promising pharmaceutical targets for a wide spectrum of human diseases - including reperfusion injury, ischemia, neurodegenerative diseases and malignant cancer (Kimura, 2010; Li et al., 2011; Olson, 2011; Quaegebeur and Carmeliet, 2010; Szabo, 2007) - the link we have established from H_2S and CYSL-1 to the inhibition of EGL-9 might lead to novel therapeutic strategies to treat these disorders.

Our analyses of the physiological function and evolution of CYSL-1 also provide surprising insights into how an ancient metabolic enzyme might have been coopted during evolution to perform a novel function in intracellular signal transduction. CYSL-1 is more closely related to bacterial and plant cysteine synthases than to animal type-II PLP-dependent enzymes. Instead of forming a CS complex with an OAS acetyltransferase, *C. elegans* CYSL-1 apparently binds the EGL-9 C-terminus via an interface derived from an ancient interaction module between OASS and SAT in plants and bacteria. Such a shift in or acquisition of a new gene function, termed "gene cooption", is a salient feature of genome evolution and can drive formation of novel biological traits that are selected (True and Carroll, 2002). Of CYSL-1 and its five *C. elegans* paralogs, ZC373.1 is more similar to eukaryotic CBS proteins, whereas CYSL-1, R08E5.2, and F59A7.9 form another homologous group related only distantly to their pro- and eukaryotic counterparts (Figure 5A). Thus, the *cysl-1* gene family might have divergently evolved and hence accommodated newly acquired functions beyond its metabolic roles in bacteria and plants. Interestingly, the expansion of the CBS protein family in nematodes and acquisition of CYSL-1-binding motifs in EGL-9 homologs appear to have co-evolved (Figure S7J) and occurred in a period approximately coincidental with anoxic H_2S release on Earth during the Permian-Triassic Mass extinction (Grice et al., 2005). Cooption of CYSL-1 from an ancient sulfide-related metabolic enzyme into a cell-signaling mediator might have had adaptive value, enabling animals to efficiently couple decreased O_2 and increased H_2S levels under hypoxia or other adverse environmental conditions with enhanced cellular protection and behavioral flexibility for better survival and reproduction.

EXPERIMENTAL PROCEDURES

EMS mutagenesis and genetic mapping

To screen for mutations that activate the HIF-1 target gene reporter *nIs470*, we mutagenized otherwise wild-type animals carrying the *K10H10.2::GFP* transgene with EMS and observed the F2 progeny using a fluorescence dissecting microscope. Animals with constitutively bright GFP fluorescence under conditions of normoxia (21% O_2) were isolated. Such mutants defined alleles of *egl-9*, *vhl-1* and *rhy-1*. To screen for suppressors of *rhy-1(n5500)*, *rhy-1(n5500) II; nIs470 IV* animals were backcrossed six times to eliminate background mutations and then mutagenized with EMS. The F2 progeny were scored to identify animals that lacked GFP expression under normoxic conditions.

To map *n5500*, the polymorphic Hawaiian CB4856 strain was crossed with *n5500; nIs470* animals to obtain F2 progeny for SNP mapping (Davis et al., 2005). To map the *n5500* suppressor *n5515* using genetic markers, *n5500 II; nIs470 IV; n5515* males were crossed with *n5500 II; nIs470 IV; dpy-6(e14) egl-15(n484) X* hermaphrodites. 7/15 Egl non-Dpy F2 progeny segregated GFP-negative *n5500*-suppressed animals. Refined mapping using SNP analysis further positioned *n5515* between *dpy-6* and *egl-15* in an interval between the SNPs pkP6127 and pkP6138. To map the dominant suppressor *n5535*, *n5500; nIs470; n5535* hermaphrodites were crossed with *n5500; nIs470* males, and GFP-positive F2 animals were isolated for SNP mapping.

Behavioral analysis and H_2S exposure

Locomotive responses to step changes of O_2 were measured using a custom-built multi-worm tracker and a gas-flow system controlled in real-time by MATLAB (See Figure S1). The gas flow consisted of pre-mixed 20%, 10%, 5%, or 0% O_2 balanced by N_2. Well-fed young adult hermaphrodites (50–100 per assay) were transferred to a Petri plate freshly seeded with the bacterium OP50 and allowed to stabilize for 1 hr before the assay at 20°C. Worm-tracking videos were analyzed later using MATLAB to calculate instantaneous

locomotion speeds and other behavioral parameters. A hypoxia chamber (Coy Laboratory) that contained 0.5% O_2 balanced by N_2 was used for experiments involving hypoxia experience. After 24 hr of hypoxia exposure, animals were allowed to recover in room air at 20°C for 2 hrs preceding the acute behavioral assay. For experiments involving H_2S exposure, 1 μl of 0.1M NaHS, an established H_2S donor that releases H_2S from solution, was dropped on the edge of agar-containing Petri plates and immediately sealed with tape to ensure airtight conditions. To obtain optimal effects, 24 hr duration of H_2S exposure was used for behavioral experiments; 12 hr duration was used for GFP induction; and 1 hr duration was used for biochemical interaction experiments and quantitative real-time PCR.

Supplementary Material

Refer to Web version on PubMed Central for supplementary material.

Acknowledgments

We thank Jo Anne Powell-Coffman, Yuichi Iino, Rene Garcia, Michael Hengartner, Mark Roth, Andy Fire and Erik Jorgensen for reagents; the *Caenorhabditis* Genetics Center for strains; Na An, Rita Droste, and Tove Ljungars for technical assistance; Ales Hnizda, Jakub Krijt and Milan Kodicek for help with characterization of purified CYSL-1; Viktor Kozich for helpful discussion; and Shunji Nakano, Takashi Hirose, Nick Paquin, Howard Chang, and Shuo Luo for comments. This work was supported by grant GM24663 to H.R.H from the NIH. R.V. was supported by grant No. 21709 from Grant Agency of Charles University, Prague, Czech Republic and by the Research Project of Charles University No. MSM0021620806. H.R.H. is an Investigator of the Howard Hughes Medical Institute and the David H. Koch Professor of Biology at MIT. N.B is supported by a National Science Foundation Graduate Research Fellowship. D.K.M. is supported by a Helen Hay Whitney Foundation postdoctoral fellowship.

REFERENCES

Aitken SM, Lodha PH, Morneau DJ. The enzymes of the transsulfuration pathways: active-site characterizations. Biochim Biophys Acta. 2011; 1814:1511–1517. [PubMed: 21435402]

Bonner ER, Cahoon RE, Knapke SM, Jez JM. Molecular basis of cysteine biosynthesis in plants: structural and functional analysis of O-acetylserine sulfhydrylase from *Arabidopsis thaliana*. J Biol Chem. 2005; 280:38803–38813. [PubMed: 16166087]

Bruick RK, McKnight SL. A conserved family of prolyl-4-hydroxylases that modify HIF. Science. 2001; 294:1337–1340. [PubMed: 11598268]

Budde MW, Roth MB. Hydrogen sulfide increases hypoxia-inducible factor 1 activity independently of von Hippel-Lindau tumor suppressor-1 in *C. elegans*. Mol Biol Cell. 2010; 21:212–217. [PubMed: 19889840]

Budde MW, Roth MB. The Response of *Caenorhabditis elegans* to Hydrogen Sulfide and Hydrogen Cyanide. Genetics. 2011

Campanini B, Speroni F, Salsi E, Cook PF, Roderick SL, Huang B, Bettati S, Mozzarelli A. Interaction of serine acetyltransferase with O-acetylserine sulfhydrylase active site: evidence from fluorescence spectroscopy. Protein Sci. 2005; 14:2115–2124. [PubMed: 15987896]

Chang AJ, Bargmann CI. Hypoxia and the HIF-1 transcriptional pathway reorganize a neuronal circuit for oxygen-dependent behavior in *Caenorhabditis elegans*. Proc Natl Acad Sci U S A. 2008; 105:7321–7326. [PubMed: 18477695]

Chen X, Jhee KH, Kruger WD. Production of the neuromodulator H2S by cystathionine beta-synthase via the condensation of cysteine and homocysteine. J Biol Chem. 2004; 279:52082–52086. [PubMed: 15520012]

Cheung BH, Arellano-Carbajal F, Rybicki I, de Bono M. Soluble guanylate cyclases act in neurons exposed to the body fluid to promote *C. elegans* aggregation behavior. Curr Biol. 2004; 14:1105–1111. [PubMed: 15203005]

Cheung BH, Cohen M, Rogers C, Albayram O, de Bono M. Experience-dependent modulation of *C. elegans* behavior by ambient oxygen. Curr Biol. 2005; 15:905–917. [PubMed: 15916947]

Darby C, Cosma CL, Thomas JH, Manoil C. Lethal paralysis of *Caenorhabditis elegans* by *Pseudomonas aeruginosa*. Proc Natl Acad Sci U S A. 1999; 96:15202–15207. [PubMed: 10611362]

Davis MW, Hammarlund M, Harrach T, Hullett P, Olsen S, Jorgensen EM. Rapid single nucleotide polymorphism mapping in *C. elegans*. BMC Genomics. 2005; 6

de Bono M, Maricq AV. Neuronal substrates of complex behaviors in *C. elegans*. Annu Rev Neurosci. 2005; 28:451–501. [PubMed: 16022603]

Demb JB. Functional circuitry of visual adaptation in the retina. J Physiol. 2008; 586:4377–4384. [PubMed: 18617564]

Epstein AC, Gleadle JM, McNeill LA, Hewitson KS, O'Rourke J, Mole DR, Mukherji M, Metzen E, Wilson MI, Dhanda A, et al. *C. elegans* EGL-9 and mammalian homologs define a family of dioxygenases that regulate HIF by prolyl hydroxylation. Cell. 2001; 107:43–54. [PubMed: 11595184]

Felix MA, Braendle C. The natural history of *Caenorhabditis elegans*. Curr Biol. 2010; 20:R965–R969. [PubMed: 21093785]

Francois JA, Kumaran S, Jez JM. Structural basis for interaction of O-acetylserine sulfhydrylase and serine acetyltransferase in the *Arabidopsis* cysteine synthase complex. Plant Cell. 2006; 18:3647–3655. [PubMed: 17194764]

Gadalla MM, Snyder SH. Hydrogen sulfide as a gasotransmitter. J Neurochem. 2010; 113:14–26. [PubMed: 20067586]

Gray JM, Hill JJ, Bargmann CI. A circuit for navigation in *Caenorhabditis elegans*. Proc Natl Acad Sci U S A. 2005; 102:3184–3191. [PubMed: 15689400]

Gray JM, Karow DS, Lu H, Chang AJ, Chang JS, Ellis RE, Marletta MA, Bargmann CI. Oxygen sensation and social feeding mediated by a *C. elegans* guanylate cyclase homologue. Nature. 2004; 430:317–322. [PubMed: 15220933]

Grice K, Cao C, Love GD, Bottcher ME, Twitchett RJ, Grosjean E, Summons RE, Turgeon SC, Dunning W, Jin Y. Photic zone euxinia during the Permian-triassic superanoxic event. Science. 2005; 307:706–709. [PubMed: 15661975]

Hsieh J, Liu J, Kostas SA, Chang C, Sternberg PW, Fire A. The RING finger/B-box factor TAM-1 and a retinoblastoma-like protein LIN-35 modulate context-dependent gene silencing in *Caenorhabditis elegans*. Genes Dev. 1999; 13:2958–2970. [PubMed: 10580003]

Hwang CS, Shemorry A, Varshavsky A. N-terminal acetylation of cellular proteins creates specific degradation signals. Science. 2010; 327:973–977. [PubMed: 20110468]

Ivan M, Haberberger T, Gervasi DC, Michelson KS, Gunzler V, Kondo K, Yang H, Sorokina I, Conaway RC, Conaway JW, et al. Biochemical purification and pharmacological inhibition of a mammalian prolyl hydroxylase acting on hypoxia-inducible factor. Proc Natl Acad Sci U S A. 2002; 99:13459–13464. [PubMed: 12351678]

Jorgensen, EM.; Rankin, C. Neural Plasticity. In: Riddle DL, BT.; Meyer, BJ.; Priess, JR., editors. C. ELEGANS II. 2nd edition. Cold Spring Harbor Laboratory Press; 1997. p. 769-790.

Kaelin WG Jr, Ratcliffe PJ. Oxygen sensing by metazoans: the central role of the HIF hydroxylase pathway. Mol Cell. 2008; 30:393–402. [PubMed: 18498744]

Kimura H. Hydrogen sulfide: from brain to gut. Antioxid Redox Signal. 2010; 12:1111–1123. [PubMed: 19803743]

Ladroue C, Carcenac R, Leporrier M, Gad S, Le Hello C, Galateau-Salle F, Feunteun J, Pouyssegur J, Richard S, Gardie B. PHD2 mutation and congenital erythrocytosis with paraganglioma. N Engl J Med. 2008; 359:2685–2692. [PubMed: 19092153]

Li L, Rose P, Moore PK. Hydrogen sulfide and cell signaling. Annu Rev Pharmacol Toxicol. 2011; 51:169–187. [PubMed: 21210746]

Liu X, Pan L, Zhuo Y, Gong Q, Rose P, Zhu Y. Hypoxia-inducible factor-1alpha is involved in the pro-angiogenic effect of hydrogen sulfide under hypoxic stress. Biol Pharm Bull. 2010; 33:1550–1554. [PubMed: 20823573]

Loor G, Schumacker PT. Role of hypoxia-inducible factor in cell survival during myocardial ischemia-reperfusion. Cell Death Differ. 2008; 15:686–690. [PubMed: 18259200]

Mazzone M, Dettori D, Leite de Oliveira R, Loges S, Schmidt T, Jonckx B, Tian YM, Lanahan AA, Pollard P, Ruiz de Almodovar C, et al. Heterozygous deficiency of PHD2 restores tumor oxygenation and inhibits metastasis via endothelial normalization. Cell. 2009; 136:839–851. [PubMed: 19217150]

McGrath PT, Rockman MV, Zimmer M, Jang H, Macosko EZ, Kruglyak L, Bargmann CI. Quantitative mapping of a digenic behavioral trait implicates globin variation in *C. elegans* sensory behaviors. Neuron. 2009; 61:692–699. [PubMed: 19285466]

Mino K, Yamanoue T, Sakiyama T, Eisaki N, Matsuyama A, Nakanishi K. Effects of bienzyme complex formation of cysteine synthetase from *Escherichia coli* on some properties and kinetics. Biosci Biotechnol Biochem. 2000; 64:1628–1640. [PubMed: 10993149]

Mozzarelli A, Bettati S, Campanini B, Salsi E, Raboni S, Singh R, Spyrakis F, Kumar VP, Cook PF. The multifaceted pyridoxal 5'-phosphate-dependent O-acetylserine sulfhydrylase. Biochim Biophys Acta. 2011; 1814:1497–1510. [PubMed: 21549222]

Mustafa AK, Gadalla MM, Sen N, Kim S, Mu W, Gazi SK, Barrow RK, Yang G, Wang R, Snyder SH. H2S signals through protein S-sulfhydration. Sci Signal. 2009; 2:ra72. [PubMed: 19903941]

Olson KR. The therapeutic potential of hydrogen sulfide: separating hype from hope. Am J Physiol Regul Integr Comp Physiol. 2011; 301:R297–R312. [PubMed: 21543637]

Olson KR, Dombkowski RA, Russell MJ, Doellman MM, Head SK, Whitfield NL, Madden JA. Hydrogen sulfide as an oxygen sensor/transducer in vertebrate hypoxic vasoconstriction and hypoxic vasodilation. J Exp Biol. 2006; 209:4011–4023. [PubMed: 17023595]

Ono B, Kijima K, Inoue T, Miyoshi S, Matsuda A, Shinoda S. Purification and properties of *Saccharomyces cerevisiae* cystathionine beta-synthase. Yeast. 1994; 10:333–339. [PubMed: 8017103]

Ozer A, Wu LC, Bruick RK. The candidate tumor suppressor ING4 represses activation of the hypoxia inducible factor (HIF). Proc Natl Acad Sci U S A. 2005; 102:7481–7486. [PubMed: 15897452]

Padilla PA, Nystul TG, Zager RA, Johnson AC, Roth MB. Dephosphorylation of cell cycle-regulated proteins correlates with anoxia-induced suspended animation in *Caenorhabditis elegans*. Mol Biol Cell. 2002; 13:1473–1483. [PubMed: 12006646]

Peng YJ, Nanduri J, Raghuraman G, Souvannakitti D, Gadalla MM, Kumar GK, Snyder SH, Prabhakar NR. H2S mediates O2 sensing in the carotid body. Proc Natl Acad Sci U S A. 2010; 107:10719–10724. [PubMed: 20556885]

Percy MJ, Zhao Q, Flores A, Harrison C, Lappin TR, Maxwell PH, McMullin MF, Lee FS. A family with erythrocytosis establishes a role for prolyl hydroxylase domain protein 2 in oxygen homeostasis. Proc Natl Acad Sci U S A. 2006; 103:654–659. [PubMed: 16407130]

Pocock R, Hobert O. Hypoxia activates a latent circuit for processing gustatory information in *C. elegans*. Nat Neurosci. 2010; 13:610–614. [PubMed: 20400959]

Powell-Coffman JA. Hypoxia signaling and resistance in *C. elegans*. Trends Endocrinol Metab. 2010; 21:435–440. [PubMed: 20335046]

Quaegebeur A, Carmeliet P. Oxygen sensing: a common crossroad in cancer and neurodegeneration. Curr Top Microbiol Immunol. 2010; 345:71–103. [PubMed: 20582529]

Rose NR, McDonough MA, King ON, Kawamura A, Schofield CJ. Inhibition of 2-oxoglutarate dependent oxygenases. Chem Soc Rev. 2011

Ruvinsky I, Ohler U, Burge CB, Ruvkun G. Detection of broadly expressed neuronal genes in *C. elegans*. Dev Biol. 2007; 302:617–626. [PubMed: 17046742]

Salsi E, Campanini B, Bettati S, Raboni S, Roderick SL, Cook PF, Mozzarelli A. A two-step process controls the formation of the bienzyme cysteine synthase complex. J Biol Chem. 2010; 285:12813–12822. [PubMed: 20164178]

Sawin ER, Ranganathan R, Horvitz HR. *C. elegans* locomotory rate is modulated by the environment through a dopaminergic pathway and by experience through a serotonergic pathway. Neuron. 2000; 26:619–631. [PubMed: 10896158]

Semenza GL. Defining the role of hypoxia-inducible factor 1 in cancer biology and therapeutics. Oncogene. 2010; 29:625–634. [PubMed: 19946328]

Shao Z, Zhang Y, Powell-Coffman JA. Two distinct roles for EGL-9 in the regulation of HIF-1-mediated gene expression in *Caenorhabditis elegans*. Genetics. 2009; 183:821–829. [PubMed: 19737748]

Shao Z, Zhang Y, Ye Q, Saldanha JN, Powell-Coffman JA. *C. elegans* SWAN-1 Binds to EGL-9 and regulates HIF-1-mediated resistance to the bacterial pathogen *Pseudomonas aeruginosa* PAO1. PLoS Pathog. 2010; 6 e1001075.

Shen C, Nettleton D, Jiang M, Kim SK, Powell-Coffman JA. Roles of the HIF-1 hypoxia-inducible factor during hypoxia response in *Caenorhabditis elegans*. J Biol Chem. 2005; 280:20580–20588. [PubMed: 15781453]

Shen C, Shao Z, Powell-Coffman JA. The *Caenorhabditis elegans rhy-1* gene inhibits HIF-1 hypoxia-inducible factor activity in a negative feedback loop that does not include *vhl-1*. Genetics. 2006; 174:1205–1214. [PubMed: 16980385]

Singh S, Padovani D, Leslie RA, Chiku T, Banerjee R. Relative contributions of cystathionine beta-synthase and gamma-cystathionase to H2S biogenesis via alternative trans-sulfuration reactions. J Biol Chem. 2009; 284:22457–22466. [PubMed: 19531479]

Szabo C. Hydrogen sulphide and its therapeutic potential. Nat Rev Drug Discov. 2007; 6:917–935. [PubMed: 17948022]

To KK, Huang LE. Suppression of hypoxia-inducible factor 1alpha (HIF-1alpha) transcriptional activity by the HIF prolyl hydroxylase EGLN1. J Biol Chem. 2005; 280:38102–38107. [PubMed: 16157596]

Trent C, Tsung N, Horvitz HR. Egg-laying defective mutants of the nematode *Caenorhabditis elegans*. Genetics. 1983; 104:619–647. [PubMed: 11813735]

True JR, Carroll SB. Gene co-option in physiological and morphological evolution. Annu Rev Cell Dev Biol. 2002; 18:53–80. [PubMed: 12142278]

Wirtz M, Droux M. Synthesis of the sulfur amino acids: cysteine and methionine. Photosynth Res. 2005; 86:345–362. [PubMed: 16307301]

Wirtz M, Heeg C, Samami AA, Ruppert T, Hell R. Enzymes of cysteine synthesis show extensive and conserved modifications patterns that include N(alpha)-terminal acetylation. Amino Acids. 2010; 39:1077–1086. [PubMed: 20658158]

Zimmer M, Gray JM, Pokala N, Chang AJ, Karow DS, Marletta MA, Hudson ML, Morton DB, Chronis N, Bargmann CI. Neurons detect increases and decreases in oxygen levels using distinct guanylate cyclases. Neuron. 2009; 61:865–879. [PubMed: 19323996]

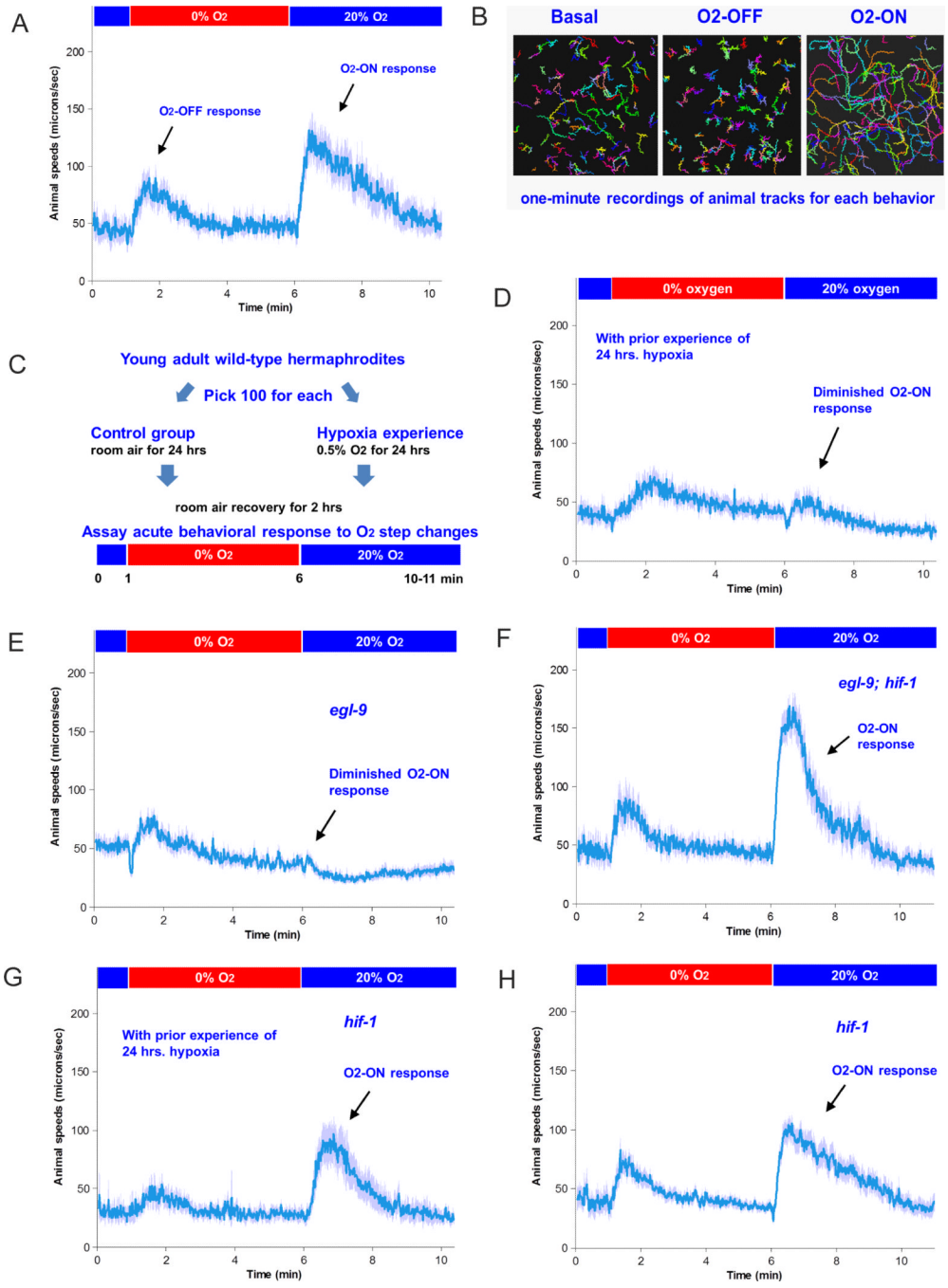

Figure 1. *C. elegans* displays O_2-associated locomotive behavioral plasticity

(A) Acute locomotive speed changes during O2-OFF and O2-ON responses. Average speed values with 2 standard errors of the means (indicated by light blue) of a population of animals (n>50) are shown with step changes of O_2 between 20% and 0% at the indicated times. The mean speed differences of all animals within 60 seconds before or after O2 restoration are highly significant ($p<0.001$, one-sided unpaired t-test; also see Supplemental Information). (B) Worm tracks showing locomotive patterns during basal state, O2-OFF and O2-ON responses. One-minute recordings were made under basal conditions (20% O2) or immediately following the initiation of O2-OFF or ON responses. (C) Schematic of behavioral paradigms used to test the effects of prior experience of hypoxia on the O2-ON

response. (D) Behavior of hypoxia-experienced wild-type animals with suppressed O2-ON response, compared to that of naive animals as shown in (A). Graphs exclusively labeled "With prior experience of 24 hrs. hypoxia" show data for hypoxia-experienced but not naive animals. (E) Behavior of *egl-9* mutants showing a lack of O2-ON response. (F) Behavior of *egl-9; hif-1* mutants with a restored O2-ON response compared to that of *egl-9* mutants. (G) Behavior of hypoxia-experienced *hif-1* mutants with a suppressed O2-ON response, compared to that of hypoxia-experienced wild-type animals. (H) Behavior of *hif-1* mutants with a normal O2-ON response.

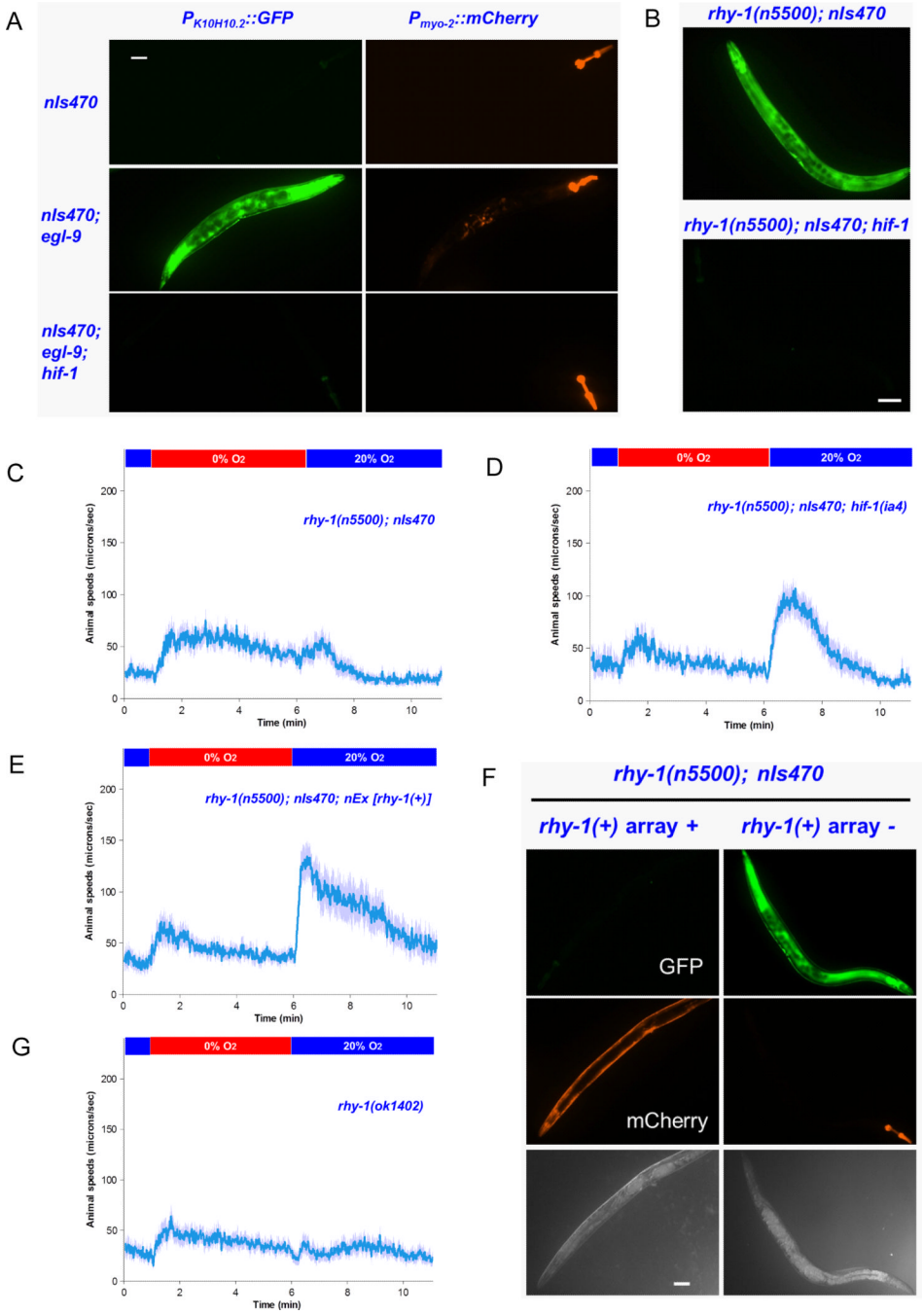

Figure 2. RHY-1 modulates HIF-1 and the O2-ON behavioral response through EGL-9

(A) Fluorescence micrographs showing constitutive GFP signals in *egl-9(−)* mutants with the transgenic reporter $P_{K10H10.2}$*::GFP* (*nIs470*), indicating high HIF-1 transcriptional activity. GFP signals are absent in the wild type and in *egl-9(sa307); hif-1(ia4)* double mutants, except for weak GFP fluorescence in the pharynx. *myo-2::mCherry* expressed in pharyngeal muscles was used as the co-injection marker. (B) *rhy-1(n5500)* mutants with strong constitutive GFP expression that is suppressed by *hif-1* mutations. (C) *rhy-1(n5500)* mutants show a defective O2-ON response. (D) *rhy-1(n5500); hif-1(ia4)* double mutants show a restored O2-ON response. (E) An extrachromasomal array containing *rhy-1(+)* genomic fragments rescues the behavioral defect in the O2-ON response of *rhy-1(n5500)*

mutants. (F) Rescued *K10H10.2::GFP* ectopic expression of *rhy-1(n5500)* mutants by *rhy-1(+)* arrays. *myo-3::mCherry* expressed in body wall muscles was the co-injection marker. (G) *rhy-1(ok1402)* null mutants show a defective O2-ON response. Scale bar: 25 μm.

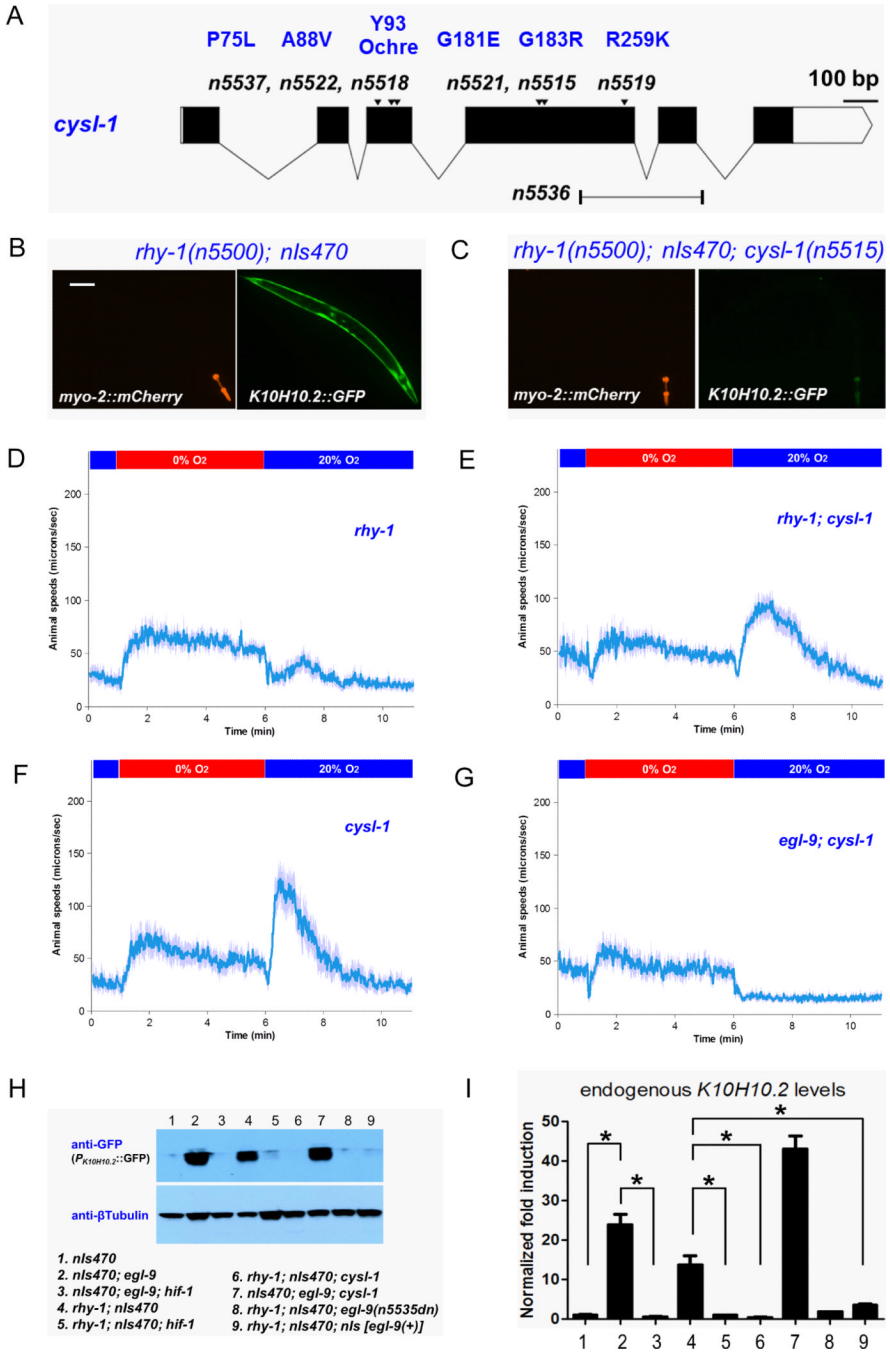

Figure 3. A modifier screen identified *cysl-1* as a regulator of HIF-1 and behavior

(A) A schematic of the *cysl-1* gene, indicating the seven alleles isolated from the *rhy-1(n5500)* suppressor screen. This drawing was generated by the Exon-Intron Graphic Maker (WormWeb.org). (B) *K10H10.2::GFP* expression in *rhy-1(n5500); nIs470* mutants with *myo-2::mCherry* as the co-injection marker. Scale bar: 25 μm. (C) *K10H10.2::GFP* expression is absent in *rhy-1(n5500); nIs470; cysl-1(n5515)* mutants. (D–E) A defective O2-ON response of *rhy-1(n5500)* mutants is suppressed by the *cysl-1(5515)* mutation. (F) *cysl-1(ok762)* null mutants show a normal O2-ON response. (G) *egl-9(sa307); cysl-1(ok762)* double mutants with a defective O2-ON response. (H) Western blots of reporter GFP expression driven by the *K10H10.2* promoter from single or multiple LOF or GOF mutants

of *rhy-1*, *cysl-1*, *egl-9* and *hif-1*. (I) Real-time PCR quantification of endogenous K10H10.2 mRNA levels (normalized to the control group of *nIs470* animals) in various mutants as indicated in (H). *: $p<0.01$, one-way ANOVA, Bonferroni post-test.

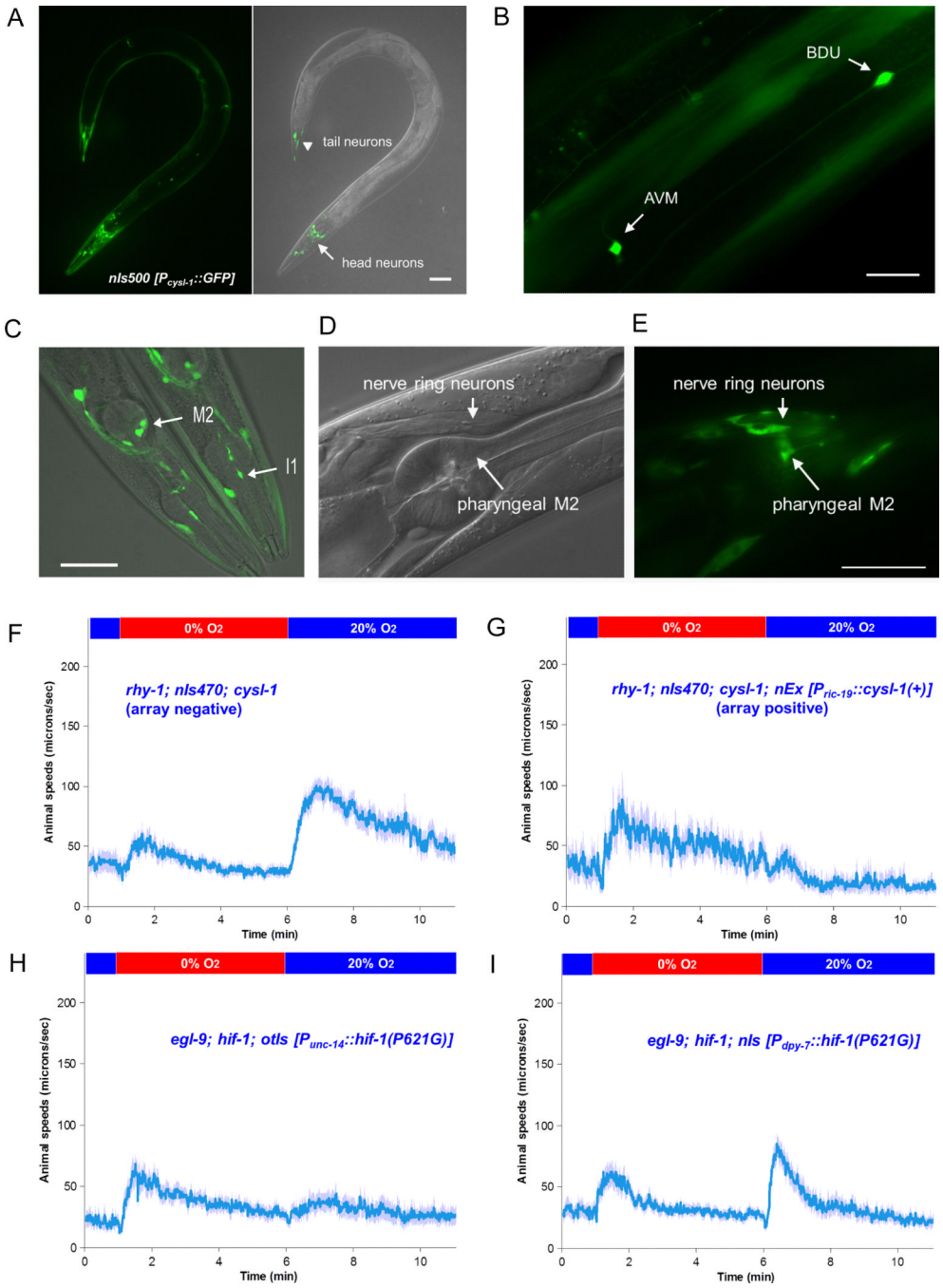

Figure 4. Expression pattern and site-of-function of CYSL-1

(A) Fluorescence and Nomarski images showing the expression pattern of *cysl-1* as visualized by the integrated transcriptional GFP reporter *nIs500*, which harbors a 2.8 kb promoter of *cysl-1* fused to GFP. Head neurons are indicated by the arrow, and tail neurons are indicated by the arrowhead. (B) Enlarged view of fluorescence micrograph showing AVM and BDU neurons. (C) Confocal microscopic view of pharyngeal (I1 and M2 indicated by arrows) and head neurons. (D–E) Expression patterns of *cysl-1* as visualized by the extrachromasomal array *nEx1838* with a translational GFP reporter harboring the promoter and genomic coding regions of *cysl-1* fused in-frame to GFP. (F–G) Rescue of *cysl-1(n5515)* phenotypes by neuronal expression of *cysl-1(+)* cDNA driven by the *ric-19*

promoter. (H) The *unc-14* promoter-driven neuronal activation of HIF-1 causes defects in the O2-ON response of *egl-9(sa307); hif-1(ia4)* double mutants. (I) The *dpy-7* promoter-driven hypodermal activation of HIF-1 does not cause defects in the O2-ON response of *egl-9; hif-1* double mutants. Scale bars: 25 μm.

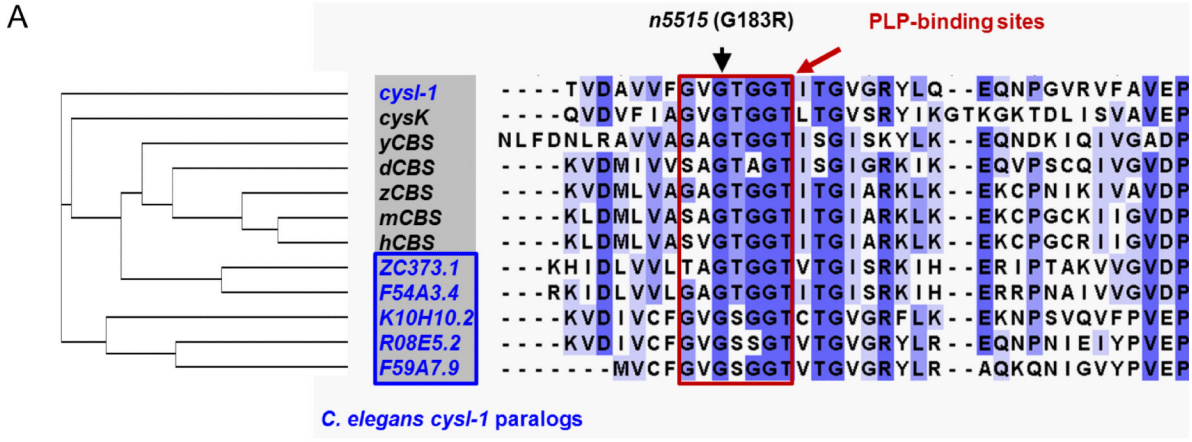

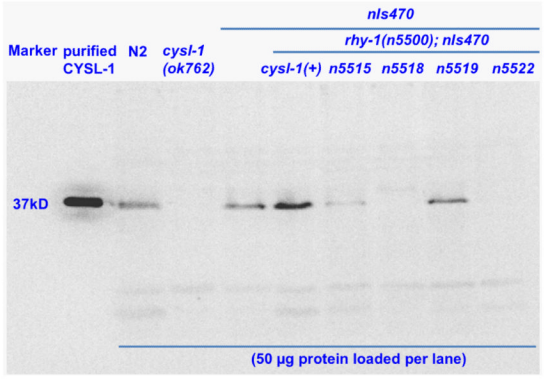

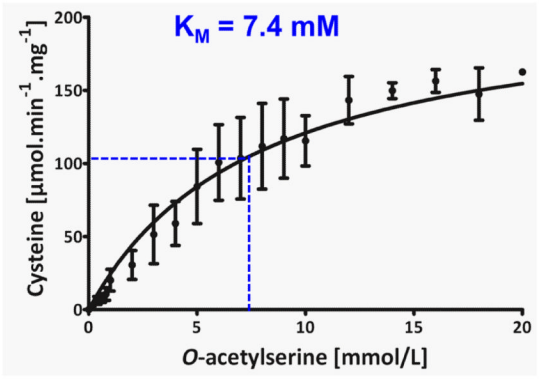

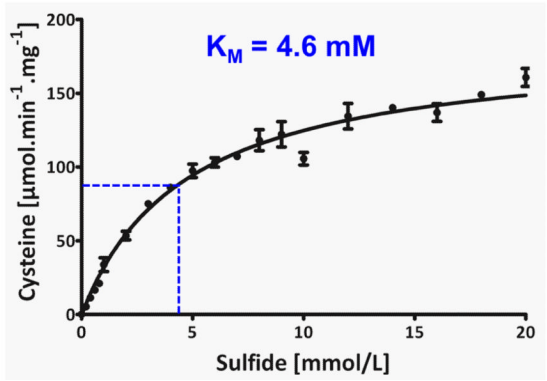

E

Organism	Enzyme	K_M for OAS [mM]	K_M for sulfide [mM]	k_{cat} [S^{-1}]
Archebacteria	*Aeropyrum pernix CS*	28.0	< 0.2	202
Bacteria	*Escherichia coli CS*	4.8	0.006	2030
	Thermus thermophilus CS	4.8	0.050	493
Plants	*Arabidopsis thaliana CS*	1.4	0.22	2170
	Spinach oleraceae CS	1.3	0.25	
Fungi	*Saccharomyces cerevisiae CBS*	1.3	16.6	19
Protazoa	*Trypanosoma cruzi CBS*	4.9	4.1	13
Nematode	***C. elegans cysl-1/C17G1.7***	**7.4**	**4.6**	**113**

Figure 5. Evolutionary and enzymatic characteristics of CYSL-1

(A) Alignment of CYSL-1 homologs identifies a highly conserved glycine disrupted by *cysl-1(n5515)*. This phylogenetic tree was generated using ClusterW2 and is displayed in a cladogram. The PLP-binding site is highlighted by the red box (Aitken et al., 2011). *C. elegans cysl-1* paralogs are indicated in the blue box. (B) Endogenous CYSL-1 protein levels as determined by SDS-PAGE and western blots and a polyclonal antibody against CYSL-1. *C. elegans* protein lysates from various genetic backgrounds were analyzed. 50 µg protein samples were loaded per lane. (C, D) Purified recombinant CYSL-1 exhibits intrinsic cysteine synthase activity. Dependence of cysteine generation on varying OAS concentration with 20 mM sulfide and varying sulfide concentration with 20 mM OAS,

respectively. Means of three measurements are shown and the Michaelis-Menten equation was used for curve fitting. Error bars represent SD. (E) K_M and k_{cat} values of CYSL-1 (determined from Figure 5C and 5D) and OAS sulfhydrylases of other species as established from previous studies (Bonner et al., 2005; Mino et al., 2000; Mozzarelli et al., 2011; Ono et al., 1994). K_M: Michaelis value, k_{cat}: turnover number.

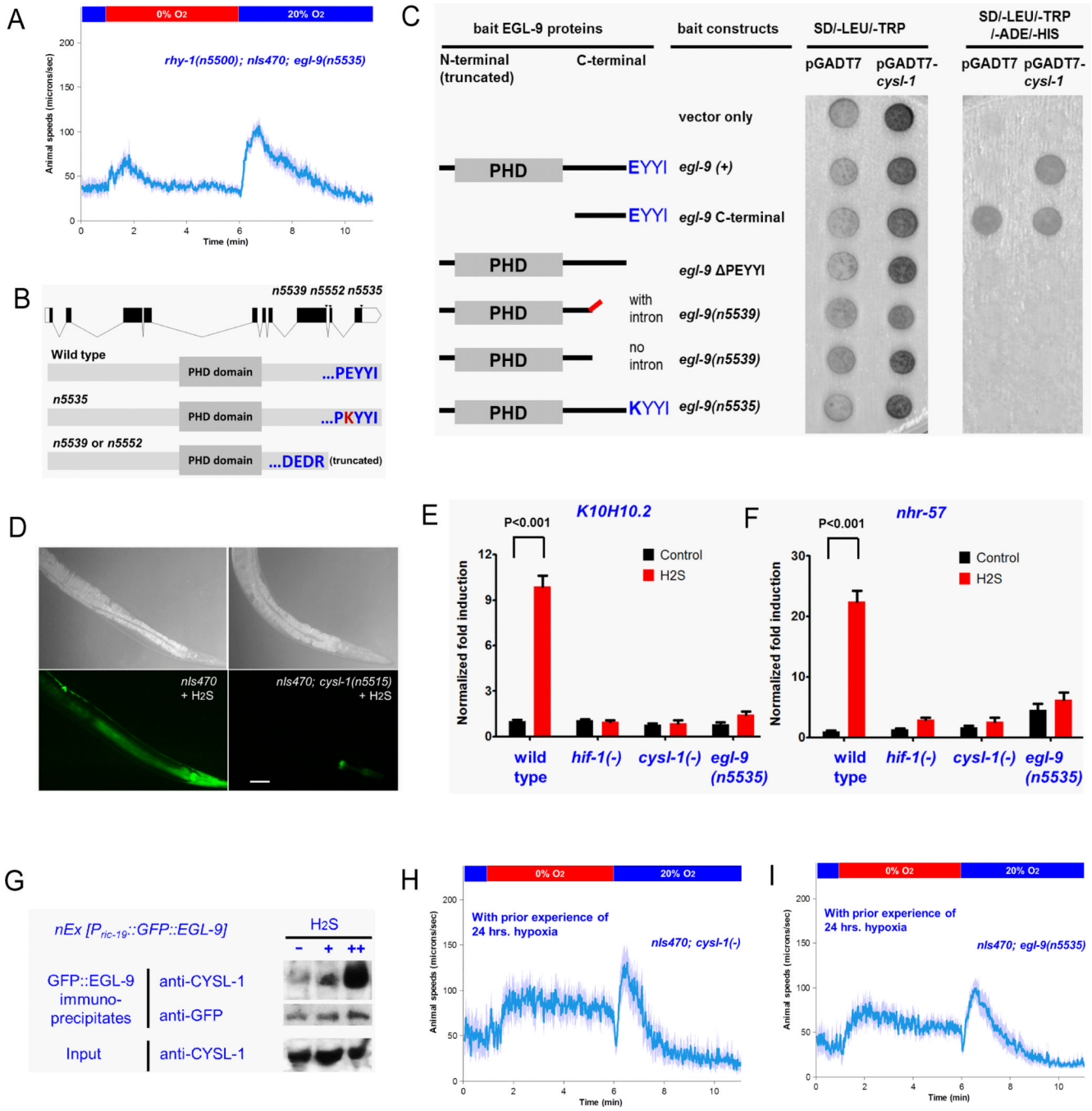

Figure 6. CYSL-1 interaction with EGL-9 mediates H_2S signaling to HIF-1 and behavioral plasticity

(A) The gain-of-function mutation *egl-9(n5535)* fully suppresses the O2-ON defect of *rhy-1(n5500)* mutants. (B) Two dominant suppressors of *rhy-1(n5500)* alter the C-terminus of EGL-9. *n5535* converts glutamic acid 720 to lysine, while *n5539* and *n5552* are splice-donor and acceptor mutations, respectively, that result in a C-terminally truncated EGL-9 protein. (C) Yeast two-hybrid assays with colony growth on selective plates (SD/-LEU/-TRP, or SD/-LEU/-TRP/-HIS3/-ADE) after co-transformation of *cysl-1* prey constructs and various *egl-9* bait constructs. The growth with vector-only control group, i.e. pGADT7 with *egl-9*-C-terminal, indicates non-specific reporter activation. All *egl-9* constructs lack the N-

terminal domain, which conferred moderate non-specific reporter activation. Note the specific association of CYSL-1 with EGL-9 with an intact C-terminus but not with *n5535* or *n5539* mutant EGL-9. (D) Exposure to low H_2S induced GFP fluorescence from the *K10H10.2::GFP* reporter in wild-type but not *cysl-1* mutant animals. Scale bars: 25 μm. (E) QPCR measurements of the endogenous HIF-1 target *K10H10.2* mRNA in the wild type and in *hif-1(ia4), cysl-1(ok762) or egl-9(n5535)* mutant backgrounds. $p<0.001$, two-way ANOVA, Bonferroni post-test. (F) QPCR measurements of the endogenous HIF-1 target *nhr-57* in the wild type and in *hif-1(ia4), cysl-1(ok762)* or *egl-9(n5535)* mutant backgrounds. (G) Protein Co-IP experiments showing that the interaction between endogenous CYSL-1 and the GFP::EGL-9 fusion protein *in vivo* is markedly enhanced by H_2S exposure. GFP-bound protein complexes isolated from lysates of the strain *nEx* [$P_{ric\text{-}19}$*::egl-9::gfp*] using anti-GFP affinity beads were analyzed by SDS-PAGE and western blots. GFP levels served as internal loading controls. (H) Behavior of *cysl-1* null mutants with decreased inhibition of the O2-ON response after 24 hr hypoxia experience as compared to hypoxia-experienced wild-type animals. (I) Behavior of *egl-9(n5535)* mutants with decreased inhibition of the O2-ON response after 24 hr hypoxia experience.

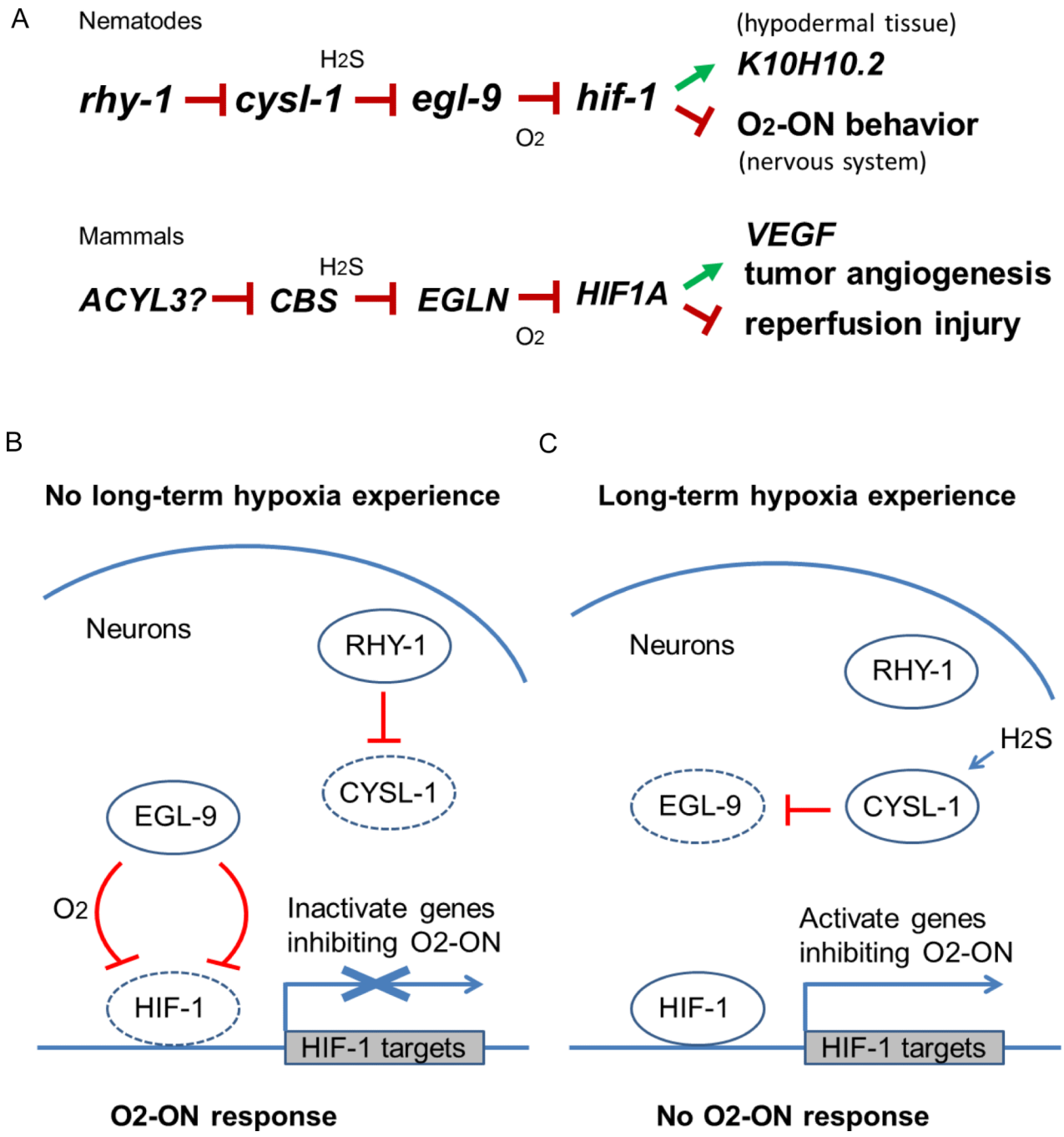

Figure 7. Models for behavioral plasticity mediated by the RHY-1/CYSL-1/EGL-9/HIF-1 pathway

(A) The genetic pathway in which *rhy-1*, *cysl-1*, and *egl-9* act in a negative-regulatory cascade to control the activity of HIF-1, which functions in neurons to modulate the O2-ON response and in the hypoderm to regulate *K10H10.2* expression. (B) Model depicting the major molecular interactions in neurons of naïve animals without experience of hypoxia, enabling the normal O2-ON response. EGL-9 promotes HIF-1 degradation (indicated by HIF-1 with dotted line) by O2-dependent hydroxylation and also inhibits HIF-1 transcriptional activity. (C) Model depicting the major molecular interactions in neurons of animals with experience of hypoxia leading to their suppressed O2-ON response. Decreased

O_2 during hypoxia impairs HIF-1 hydroxylation, which stabilizes HIF-1 but alone is not sufficient to activate HIF-1 targets. Hypoxia also increases H_2S levels to promote CYSL-1 sequestration of EGL-9, thus alleviating inhibition of HIF-1 transcriptional activity. EGL-9 inactivation (indicated with dotted line) by the dual regulatory mechanisms drives HIF-1 activation. See text for details.

TABLE 1

(A) *rhy-1(n5500)* suppressors

Chr.	Alleles	Phenotype	Genes
V	*n5513, n5527*	Recessive	***hif-1***
V	*n5512, n5514, n5516, n5538, n5541*	Recessive	***tam-1***
V	*n5535, n5539, n5552*	Dominant	***egl-9***
X	*n5515, n5518, n5519, n5521, n5522, n5536, n5537*	Recessive	***cysl-1 (C17G1.7)***

(B) *cysl-1* alleles from *rhy-1(n5500)* suppressor screen

Genotype	GFP	O2-ON response	Mutation	a.a. change
nIs470 IV	0%	Normal		
n5500 II; nIs470 IV	100%	Defective		
n5500 II; nIs470 IV; n5515 X	0%	Normal	GGA->AGA	G183R
n5500 II; nIs470 IV; n5518 X	0%	Normal	TAT->TAA	Y93Ochre
n5500 II; nIs470 IV; n5519 X	0%	Normal	AGA->AAA	R259K
n5500 II; nIs470 IV; n5522 X	0%	Normal	GCT->GTT	A88V
n5500 II; nIs470 IV; n5521 X	0%	Normal	GGG->GAG	G181E
n5500 II; nIs470 IV; n5537 X	0%	Normal	CCA->CTA	P75L
n5500 II; nIs470 IV; n5536 X	0%	Normal	deletion	

(C) Epistatic analysis of the RHY-1/CYSL-1/EGL-9/HIF-1 pathway

Genotype	GFP	O2-ON response
nIs470; egl-9(n586)	100%	Defective
nIs470; rhy-1(n5500)	100%	Defective
nIs470; hif-1(ia4)	0%	Normal
nIs470; cysl-1(ok762)	0%	Normal
nIs470; egl-9(n586); hif-1(ia4)	0%	Normal
nIs470; rhy-1(ok1402); hif-1(ia4)	0%	Normal
nIs470; rhy-1(ok1402); cysl-1(ok762)	0%	Normal
nIs470; egl-9(sa307); cysl-1(ok762)	100%	Defective
nIs470; rhy-1(n5500); nIs [egl-9(+)]	0%	Normal
nIs470; egl-9(n586); nEx [rhy-1(+)]	100%	Defective